A Single Molecule Perspective on the Functional Diversity of *in Vitro* Evolved β-Glucuronidase

Raphaela B. Liebherr,[†] Max Renner,[‡] and Hans H. Gorris*,[†]

[†]Institute of Analytical Chemistry, Chemo- and Biosensors and [‡]Institute of Biophysics and Physical Biochemistry, University of Regensburg, 93040 Regensburg, Germany

S *Supporting Information*

ABSTRACT: The mechanisms that drive the evolution of new enzyme activity have been investigated by comparing the kinetics of wild-type and *in vitro* evolved β-glucuronidase (GUS) at the single molecule level. Several hundred single GUS molecules were separated in large arrays of 62 500 ultrasmall reaction chambers etched into the surface of a fused silica slide to observe their individual substrate turnover rates in parallel by fluorescence microscopy. Individual GUS molecules feature long-lived but divergent activity states, and their mean activity is consistent with classic Michaelis–Menten kinetics. The large number of single molecule substrate turnover rates is representative of the activity distribution within an entire enzyme population. Partially evolved GUS displays a much broader activity distribution among individual enzyme molecules than wild-type GUS. The broader activity distribution indicates a functional division of work between individual molecules in a population of partially evolved enzymes that—as so-called generalists—are characterized by their promiscuous activity with many different substrates.
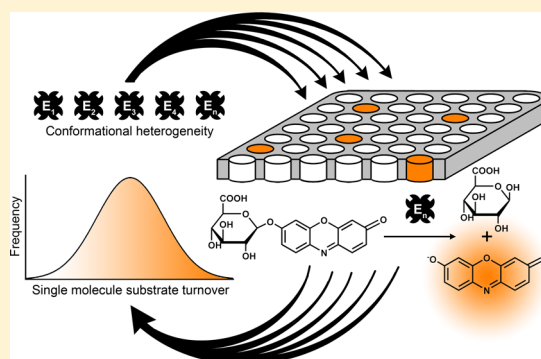
INTRODUCTION

Analyzing the catalytic mechanisms of enzymes and their evolution is crucial to understanding the biochemical reactions of life. Exactly 100 years ago, the landmark work of Michaelis and Menten provided a conceptual framework for analyzing enzyme kinetics in bulk solution.[1] The functional heterogeneity in an enzyme population, however, cannot be resolved by employing classic bulk reactions. Therefore, the implementation of new single molecule technologies has enabled a more detailed description of enzyme reactions. For example, single molecule experiments have revealed dynamic disorder in subsequent catalytic cycles of cholesterol oxidase,[2] horseradish peroxidase,[3] lipase B,[4,5] β-galactosidase from *Escherichia coli*,[6] and bovine α-trypsin.[7,8]

Instead of observing single substrate turnover events of only one or a few, typically surface-immobilized enzyme molecules, many individual enzyme molecules can be separated and monitored free in solution in femtoliter (μm³)-sized reaction chambers such as water-in-oil droplets,[9] liposomes,[10] or femtoliter arrays etched into optical fiber bundles,[11] planar glass slides,[12] or molded into PDMS.[13] In particular, femtoliter arrays etched into the surface of glass provide large numbers of rigid and homogeneous reaction chambers for enclosing and observing several hundred individual enzyme molecules in parallel.[14] The high degree of parallelization ensures excellent statistics on the static heterogeneity in an enzyme population. In addition to the single enzyme molecule, a large excess of fluorogenic substrate is present in the femtoliter chambers. Thus, the integrated product formation of many subsequent

catalytic cycles can be recorded in individual chambers by fluorescence microscopy over long periods of time. In this way, it has been shown that individual molecules of the hydrolytic enzyme β-galactosidase[13,15,16]—as well as other enzymes[12,17,18]—possess distinct and long-lived activity states. The average turnover rates of individual β-galactosidase molecules enclosed in femtoliter arrays exhibit essentially the same dependence on the substrate concentration as the respective bulk reactions. More importantly, these single molecule experiments revealed a broad activity distribution with a coefficient of variation of about 30%, which notably is the same for all substrate concentrations investigated up to 150 μM.[15]

β-Galactosidase and β-glucuronidase (GUS) from *E. coli* catalyze the hydrolysis of very similar glycosidic substrates. Both enzymes are only active as homotetramers because their active sites contain elements of two neighboring monomers as revealed by the crystal structure (Figure 1A).[19,20] The genes of these enzymes diverged from an ancient common ancestor.[21] Over the course of evolution, GUS has acquired a different amino acid sequence and with 273 kDa[22] is approximately only half the size of β-galactosidase. Matsumura and Ellington[23] showed that the native substrate specificity of wild-type GUS can be converted to 50 million-fold higher β-galactosidase activity by *in vitro* evolution within a few rounds of mutation and screening. This study also revealed that the inversion of
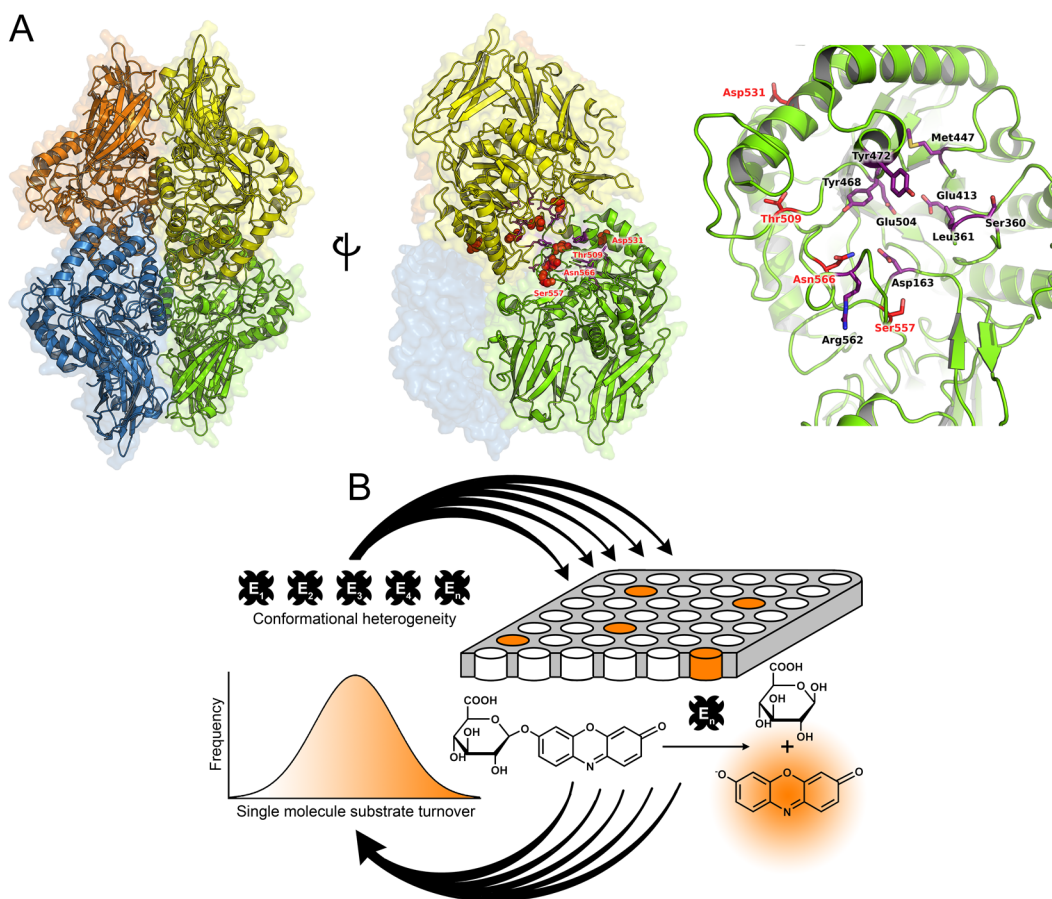
Figure 1. Single molecule analysis of β-glucuronidase (GUS). (A) Crystal structure of the *E. coli* GUS tetramer (left) and the interface of two monomers (center) rendered with PyMOL (PDB ID: 3k46). Four amino acid positions that are mutated in partially evolved GUS variant T509A/D531E/S557P/N566S are highlighted in red. The right panel shows the positions of the mutated amino acids relative to the active center. (B) Individual molecules of a conformationally heterogeneous enzyme population ($E_1 - E_n$) are isolated in an array of 62 500 femtoliter chambers etched into the surface of a fused silica slide. The array is fastened in a custom-built holder on top of an inverted fluorescence microscope and tightly sealed by a gasket under mechanical pressure (gasket not shown). Individual GUS molecules hydrolyze the nonfluorescent substrate ReG to fluorescent resorufin, which emits orange light. The substrate turnover of hundreds of individual GUS molecules is recorded in separate femtoliter chambers by wide-field fluorescence microscopy. Individual trajectories of the substrate turnover are then assembled as histograms to expose the activity distribution within the enzyme population.

GUS activity proceeds through nonspecific intermediates (or generalists) that keep their wild-type activity but also accept a broad range of other glycosidic substrates. After passing through the nonspecific intermediates, a specialized mutant GUS emerges that looses its native activity and is specific for galactopyranoside substrates. Tawfik and colleagues[24] generalized this observation to many other types of enzymes and showed that it is a general principle of adaptive evolution. The broad range of substrates catalyzed by a generalist—its so-called promiscuous activity—has been explained by a higher diversity of conformational states.[25] The high conformational plasticity of the generalists can serve as an evolutionary starting point for adopting new enzyme functions.

The conformational diversity of evolved enzymes has been analyzed, e.g., by X-ray crystallography, NMR, and pre-steady-state kinetics.[26,27] Essentially all information on their promiscuous activity has been derived from studies in bulk solution that do not reveal how the higher conformational diversity affects the substrate turnover of individual enzyme molecules. Here, we have addressed this question by enclosing wild-type β-glucuronidase and *in vitro* partially evolved β-glucuronidase in large femtoliter arrays to compare their

substrate turnover rates at the single molecule level (Figure 1B).

■ EXPERIMENTAL SECTION

Protein Expression and Purification. Expression plasmids pET-28a(+) containing sequences for N-terminally his-tagged wild-type β-glucuronidase (GUS) or the partially evolved variant T509A/D531E/S557P/N566S were kind gifts of Ichiro Matsumura and have been previously described.[23] The plasmids were used to transform *Escherichia coli* T7 Express cells (New England Biolabs, www.neb.com). For protein production, the transformed cells were cultivated in 1 L batches of Luria–Bertani (LB) medium at 37 °C in the presence of kanamycin (25 μg/mL). Protein expression was induced at an OD_{600} (optical density at 600 nm) of 0.4–0.6 by adding 0.5 mM of isopropyl-β-D-thiogalactopyranosid (IPTG) to the culture medium. The bacteria were then cultivated at 37 °C for further 16 h and harvested by centrifugation at 4 °C for 20 min at 3000 × *g*. The cell pellets were resuspended in 20 mL of nickel chelate chromatography running buffer (50 mM sodium phosphate, pH 7.0, 300 mM NaCl, 10 mM imidazole, 5 mM β-mercaptoethanol, 1 mM EDTA) per liter medium. Cell disruption was carried out by sonication and followed by pelleting via centrifugation at 4 °C for 30 min at 23 000 × *g*. The supernatant was loaded on a pre-equilibrated HisTrap FF crude affinity column (GE Healthcare, www.gehealthcare.com) and eluted by

linearly increasing the imidazole concentration of the running buffer. The recombinant proteins were further purified by size exclusion chromatography (SEC) using a S200 26/60 column (GE Healthcare) pre-equilibrated in SEC running buffer (50 mM sodium phosphate, pH 7.0, 300 mM NaCl). The purity of the resulting protein preparations was confirmed by SDS-PAGE and protein concentrations were determined by Bradford assay[28] or absorption spectroscopy.[29] Purified proteins were concentrated using Amicon Ultra 4 centrifugal units (Millipore, www.millipore.com). Droplets of the protein solution were snap-frozen in liquid nitrogen and stored at −80 °C. Buffer exchanges prior to kinetic experiments were carried out using NAP-10 columns (GE Healthcare).

Fabrication of Femtoliter Arrays and Gasket. Femtoliter arrays were microstructured into the surface of a fused silica wafer by photolithography and anisotropic reactive ion etching as described in the Supporting Information. The arrays consisted of 250×250 (62 500) cylindrical wells with a diameter of 4 μm and a depth of 3 μm defining a volume of 38 μm^3 (or femtoliters) as confirmed by scanning electron microscopy (SI Figure 1). The wells were arranged in a rectangular lattice with a pitch of 10 μm, resulting in an overall edge length of 2.5×2.5 mm^2. The wafer was cut into slides of 1.5×1.5 cm^2 such that a single array was located in the middle of each slide. The femtoliter arrays were used repeatedly and before each experiment they were first cleaned with piranha solution (1:3 ratio of 30% H$_2$O$_2$ and conc. H$_2$SO$_4$) for 20 min, then immersed in distilled water for 10 min, sonicated for another 15 min, and finally air-dried. The femtoliter arrays were sealed by using a polydimethylsiloxane (PDMS) gasket (SYLGARD 184 silicone elastomer kit, Dow Corning, www.dowcorning.com). A 0.5-mm-high layer of PDMS was cast on a clean and smooth surface. After curing at 37 °C for 48 h, the PDMS was cut into pieces of 5×5 mm^2. A new piece of PDMS was used for each experiment, cleaned with curd soap, and bidistilled water.

Buffers and Reagents for Enzyme Kinetic Experiments. Stock solutions of the fluorogenic substrate resorufin β-D-glucuronide (5 mM) (ReG, Sigma-Aldrich, www.sigmaaldrich.com) in dimethyl sulfoxide (DMSO) and 200 μM resorufin, sodium salt, (Invitrogen, www.invitrogen.com) in DMSO were aliquoted and stored at −20 °C. All dilution steps as well as the enzyme reactions were carried out at room temperature in either GUS buffer (50 mM sodium phosphate, pH 7.0, 5 mM β-mercaptoethanol, 1 mM EDTA) or phosphate buffered saline (PBS: 2.7 mM KCl, 2 mM KH$_2$PO$_4$, 137 mM NaCl, 10 mM Na$_2$HPO$_4$, pH 7.4) containing 0.05 mg/mL bovine serum albumin (BSA, Sigma-Aldrich).

Single Enzyme Molecule Experiments. For all single molecule experiments the room temperature was maintained at 22 °C with air conditioning. A femtoliter array was fastened in a custom-built array holder and mounted on an inverted epi-fluorescence microscope (Eclipse Ti-E, Nikon, www.nikoninstruments.com). The fluorogenic substrate ReG and GUS were diluted in PBS buffer and mixed just before an experiment was started. Varying concentrations of ReG and approximately 1.8 pM of GUS were prepared and filled into the wells by dispensing 5 μL of the reaction mixture on the array. The array was covered by the PDMS gasket. A torque screwdriver was used to apply mechanical pressure of 2.5 to 3.0 cNm on the PDMS gasket, thus tightly sealing the array. The Poisson distribution $P_\mu(x) = e^{-\mu}\mu^x/x!$, where μ is the average number of enzyme molecules per chamber, indicates the probability $P_\mu(x)$ that exactly x enzyme molecules are enclosed in a given chamber. An enzyme concentration of 1.8 pM enzyme in a volume of 38 fL yields a ratio of one enzyme molecule in 20 chambers ($\mu = 0.05$). Under these conditions, most chambers remain empty ($P_{0.05}(0) = 0.95$), 5% contain only a single enzyme molecule ($P_{0.05}(1) = 0.05$), and the probability that there are more than one single enzyme molecule in a chamber is very low ($P_{0.05}(>1) < 0.001$).

Image Acquisition and Analysis. The image acquisition was started within 2 min after mixing enzyme and substrate. The fluorescence intensity in individual chambers of the femtoliter array was monitored over time through the opposite face of the glass slide by wide-field fluorescence microscopy. Images were acquired every 30 s using an exposure time of 200 ms (neutral density filter: ND 4) for at least 5 min on the inverted epifluorescence microscope equipped with a precentered fiber-optical mercury illuminator (Intensilight, Nikon), a 20× objective (CFI60 Plan Apo, NA 0.75, Nikon), a filter set for resorufin (λ_{ex} = 577 ± 10 nm, λ_{em} = 620 ± 60 nm, Chroma Technology, www.chroma.com) and a sensitive, high resolution (5.5 megapixels) sCMOS-camera cooled to −31 °C (Andor Technology, www.andor.com). About 5000 femtoliter chambers were in the field of view of the microscope. The software NIS-Elements (Nikon) was used to control image acquisition, retrieve the fluorescence signals from individual chambers, and process the images. The fluorescence increase generated by individual enzyme molecules was background-corrected by subtracting the fluorescence intensity of chambers containing no enzyme and calibrated by determining the fluorescence intensity of resorufin standard solutions filled into the femtoliter array (SI Figure 2A). Enzyme kinetics was analyzed by using GraphPad Prism 5 (www.graphpad.com).

Bulk Enzyme Experiments. The bulk activity of GUS was determined in transparent 96-well microtiter plates (Nunc, www.nuncbrand.com) under the same reaction conditions as in the single molecule experiment. A bulk enzyme concentration of 36 pM equals a single enzyme molecule in a volume of 38 fL. The substrate turnover of various ReG concentrations was monitored on a microtiter plate reader (Fluostar Optima, bMG-Labtech, www.bmglabtech.com) (λ_{ex} = 544 nm, λ_{em} = 575 nm) and calibrated by determining the fluorescence intensities of resorufin standard solutions (SI Figure 2B).

■ RESULTS AND DISCUSSION

Optimizing the Reaction Conditions for Detecting Single Molecules of β-Glucuronidase (GUS). The his-tagged GUS expressed in *E. coli* was highly purified by nickel chelate chromatography and subsequent size exclusion chromatography (SI Figure 3). Substrate saturation curves were obtained with the chromogenic substrate *para*-nitrophenyl (pNP) glucuronide because it is soluble in aqueous buffers up to a millimolar concentration range (SI Figures 4 and 5). Wild-type GUS has a high catalytic efficiency ($k_{cat}/K_M = 8.9 \times 10^5$ s^{-1} M^{-1}) as described earlier[23] (SI Table 1). Additionally, we analyzed a partially evolved GUS variant containing four amino acid substitutions (T509A/D531E/S557P/N566S) that keeps the original high activity for pNP glucuronide ($k_{cat}/K_M = 8.3 \times 10^4$ s^{-1} M^{-1}) but also catalyzes the turnover of a broad range of other glycosidic substrates.[23]

The chromogenic reaction of pNP glucuronide, however, is not sensitive enough to report the activity of single GUS molecules. Thus, we compared the hydrolysis of pNP glucuronide with the respective fluorogenic substrate resorufin β-D-glucuronide (ReG), which releases the highly fluorescent product resorufin. The original GUS buffer system[23] was replaced by phosphate-buffered saline (PBS) containing BSA for blocking nonspecific binding. The reaction in PBS enables a direct comparison with the single molecule reaction of β-galactosidase.[15] The change of substrate and buffer led to a small increase in k_{cat}/K_M (wild-type GUS: 1.6×10^6 s^{-1} M^{-1}; partially evolved GUS: 9.3×10^4 s^{-1} M^{-1}). The substrate turnover of wild-type GUS shows a typical hyperbolic dependency in a concentration range between 12.5 and 150 μM ReG (Figure 2). Due to the limited solubility of ReG in aqueous buffer, concentrations higher than 150 μM could not be used. For the same reason, it was not possible to perform a Michaelis−Menten analysis of partially evolved GUS (K_M = 1260 μM in the reaction with pNP glucuronide, SI Table 1).

Analyzing Wild-Type GUS at the Single Molecule Level. The static heterogeneity of an enzyme population can be analyzed by enclosing hundreds of single enzyme molecules in large arrays of femtoliter-sized chambers.[15] Femtoliter arrays
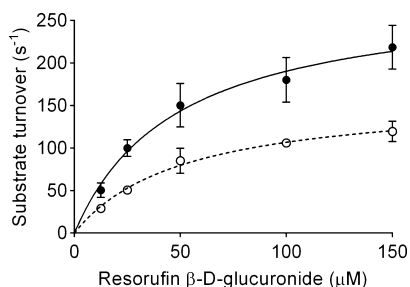
Figure 2. Substrate saturation curves of wild-type GUS. Empty circles indicate the average activity and standard deviation of three bulk experiments (K_M = 52 ± 8 μM; k_{cat} = 162 ± 10 s^{-1}), and full circles the average activity and standard deviation of six independent single molecule experiments (K_M = 49 ± 8 μM; k_{cat} = 283 ± 19 s^{-1}).

etched into the surface of a fused silica slide were filled with 1.8 pM of GUS, which yields a single GUS molecule in every twentieth chamber according to Poisson statistics (Figure 1). Additionally, the chambers contained at least 12.5 μM—or 3 million molecules in a volume of 38 fL—of the substrate ReG. Under these conditions, wild-type GUS hydrolyses ReG with an average turnover rate of 50 s^{-1} and there is less than 1% substrate depletion after a reaction time of 5 min. The fluorescence intensity of the accumulating product resorufin was recorded simultaneously by wide-field fluorescence microscopy in more than 100 chambers that contained a single GUS molecule. Nonspecific binding of the enzyme to the surface of the femtoliter chambers was efficiently blocked by adding BSA to the PBS buffer as described earlier.[15]

Figure 3A shows a small section of the large femtoliter array 1, 2.5, and 5 min after sealing the chambers. Four "active" chambers that contain a single molecule of wild-type GUS and one "inactive" chamber that contains only substrate without enzyme are highlighted. The trajectories of these chambers are shown in Figure 3B. The fluorescence intensity in chambers without enzyme is constant over the whole experiment and served for background correction (SI Table 2). By contrast,

chambers that contain a single GUS molecule produce a constant amount of resorufin over time. Furthermore, the single molecule approach in femtoliter arrays also reveals that the substrate turnover differs among individual enzyme molecules, which conforms to the static heterogeneity observed earlier for β-galactosidase.[15] The averaged trajectories of several hundred individual molecules of wild-type GUS assembled from three independent measurements are summarized in Figure 3C. Their slope strongly depends on the substrate concentration in the range of 12.5 to 150 μM and is consistent with Michaelis−Menten kinetics in bulk reaction.

The turnover rates of several hundred trajectories observed at different substrate concentrations are plotted as histograms in Figure 4. In some histograms a very small subpopulation is detectable, which is on average twice as active as the main population and can be attributed to a few chambers containing two enzyme molecules. This small subpopulation, however, can be readily separated from the majority of single molecule trajectories that follow a Gaussian distribution. The mean activity calculated from single molecule trajectories is higher than the activity of the bulk reaction because it is not possible to completely prevent an inactive fraction of GUS (e.g., resulting from tetramer dissociation) in the expression and purification steps. While a fraction of inactive enzymes would lead to an apparent decrease in the substrate turnover rates calculated from a bulk reaction, in femtoliter arrays only active enzyme molecules are included in the activity calculation.[14] The substrate saturation curves of the bulk and the mean single molecule reactions (Figure 2) yield essentially the same K_M of about 50 μM because K_M is independent of the enzyme concentration. In contrast, k_{cat} ($v_{max}/[E]_0$ = 162 s^{-1}) calculated from a bulk reaction is lower than k_{cat} determined directly from single molecule substrate turnover trajectories (283 s^{-1}).

The activity distribution determined from the Gaussian distribution is largely constant (CV ∼ 20%) for substrate concentrations between 25 μM and 150 μM (Figure 4). A slightly broader activity distribution (25%) is observed at low substrate concentrations of 12.5 μM, which can be attributed to
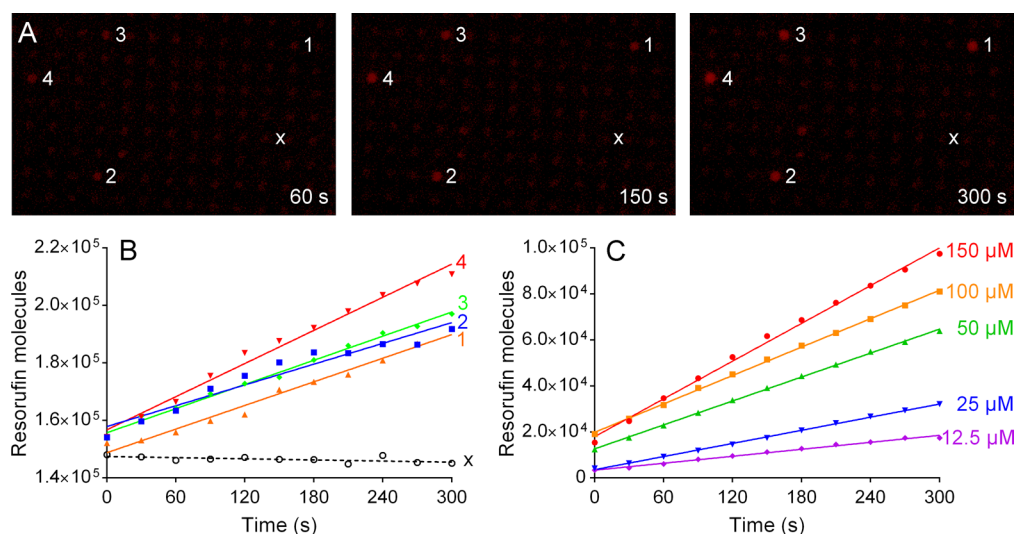
Figure 3. Single molecule substrate turnover of wild-type GUS. (A) wild-type GUS (1.8 pM) was enclosed with 100 μM of ReG in the femtoliter array and images were acquired every 30 s by wide-field fluorescence microscopy (SI Video). (B) Product formation in four active and one inactive chamber (x) indicated in (A) is plotted against time. While the background fluorescence (x) is constant over time, single molecules of wild-type GUS exhibit individually different trajectories. (C) Several hundred background-corrected trajectories of single GUS molecules are composed to ensemble trajectories that are strongly dependent on the substrate concentration as expected from a classical Michaelis−Menten reaction.
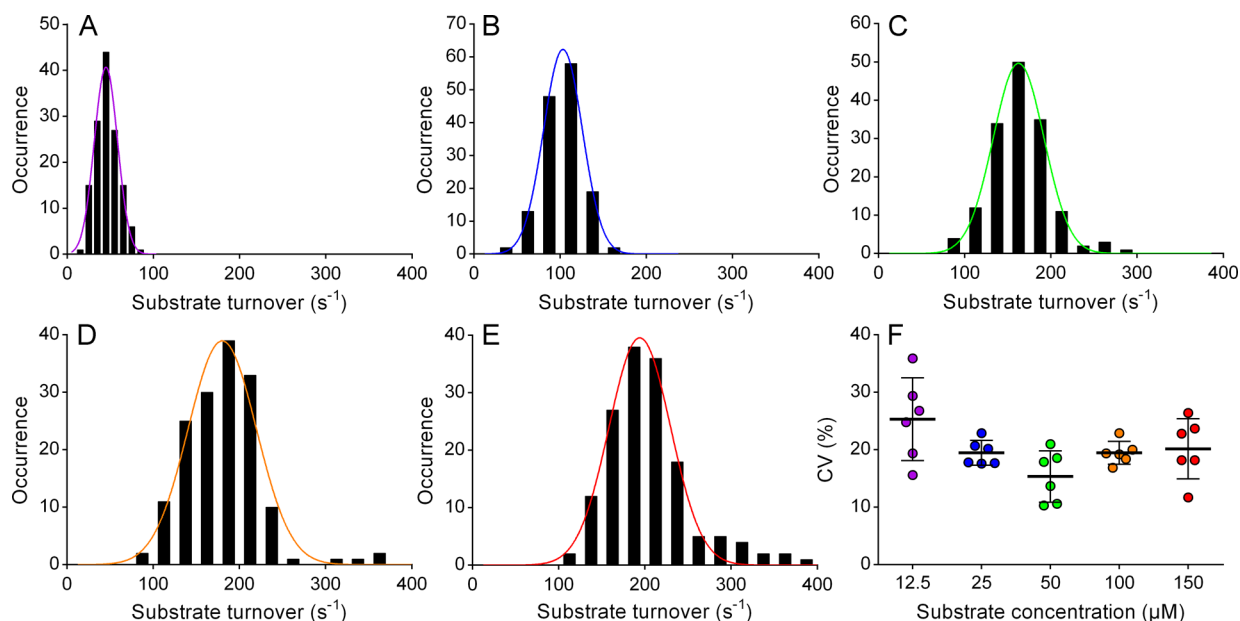
Figure 4. Single molecule substrate turnover distribution of wild-type GUS. Each histogram shows a representative femtoliter array experiment recorded for 5 min at a substrate concentration of (A) 12.5 μM, (B) 25 μM, (C) 50 μM, (D) 100 μM, and (E) 150 μM. A bin time of 10 s^{-1} was used for (A) and 25 s^{-1} for (B−E). The activity distribution in each histogram follows a Gaussian distribution. (F) Coefficient of variations (CV) calculated from the Gaussian distributions (CV = standard deviation/mean) of six independent experiments.
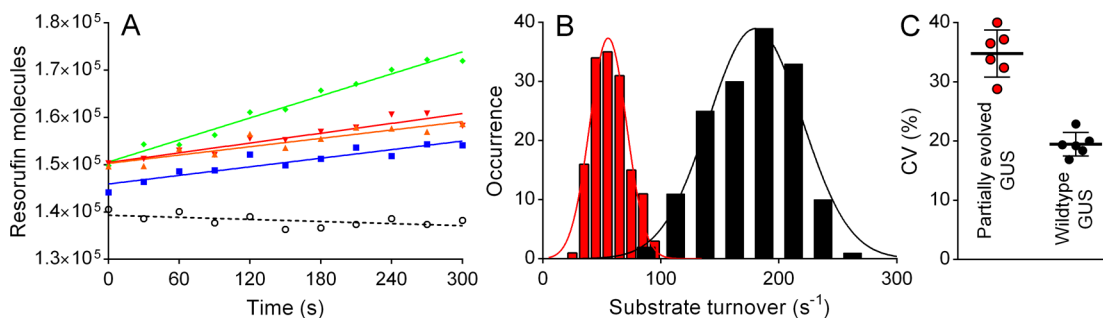
Figure 5. Differences in the single molecule substrate turnover distribution between wild-type GUS and partially evolved GUS variant T509A/D531E/S557P/N566S (100 μM substrate concentration). (A) Single molecule trajectories of partially evolved GUS. (B) The substrate turnover histograms of partially evolved GUS (red, bin time: 10 s) and wild-type GUS (black, bin time: 25 s) both follow a Gaussian distribution. (C) Coefficient of variations (CV) calculated from the Gaussian distributions (CV = standard deviation/mean) of six independent experiments. The activity of partially evolved GUS (CV = 35%) is significantly more broadly distributed among individual molecules than the respective activity of wild-type GUS (CV = 20%) (unpaired t test, $p \leq 0.0001$).

low intensity trajectories and thus higher background noise. We compared the activity distribution of GUS with β-galactosidase, which is more than twice as active as GUS. Both enzymes display an activity distribution that is largely independent of the substrate concentration. Thus, the activity distribution can be related to differences in k_{cat} rather than K_M as described earlier.[15] β-Galactosidase, however, shows a broader activity distribution (CV = 30%) than GUS. There are several reasons that may be implicated in the broader activity distribution of β-galactosidase. (1) β-Galactosidase is twice as large as GUS and thus can adopt a larger conformational space. (2) β-Galactosidase binds two Mg^{2+} ions per monomer, which can be a source of metal heterogeneity;[30] GUS, however, binds no metal ions. (3) β-Galactosidase has three catalytic functions:[31] β-galactosidase not only hydrolyzes its natural substrate lactose to galactose and glucose but to the same extent (~50%) also performs a transgalactosylation reaction on lactose to generate allolactose. Allolactose binds to the *lac* repressor of the *lacZ* gene and thus induces the *lac* operon and results in the

expression of β-galactosidase. As a third function, β-galactosidase converts allolactose to the monosaccharides. These three functions may require that β-galactosidase adopts more conformational states. By contrast, β-glucuronides can induce the expression of GUS directly[32] and the hydrolysis of β-glucuronides is the only known natural function of GUS.

Single Molecule Analysis of Molecular Evolution. The *in vitro* evolution of enzymes proceeds via so-called generalists that keep their original wild-type activity but also accept a broad range of other substrates before an enzyme can acquire a high activity and specificity for a new substrate.[24] The broad range of substrates accepted by the generalist has been explained by a higher conformational plasticity such that one conformation carries out the native function and an alternative conformation is able to carry out a promiscuous function. So far, however, all experiments showing a higher conformational plasticity of partially evolved enzymes were performed in bulk solution where the contribution of individual enzyme molecules remains hidden.

Here, we separated and analyzed several hundred individual molecules of a partially evolved GUS variant T509A/D531E/S557P/N566S in femtoliter chambers under the same reaction conditions as wild-type GUS. This partially evolved GUS was identified during the *in vitro* evolution of wild-type GUS toward a higher β-galactoside activity in the second round of screening by Matsumura et al.[23] It contains four amino acid substitutions highlighted in red in Figure 1A. Three substitutions are located in active-site loops while D531E is located in a solvent-exposed α-helix and was reported to have no functional effect.[23] This partially evolved GUS shows the characteristic properties of a generalist: it is still highly active toward glucuronide substrates but additionally hydrolyzes many other glycosidic substrates.[23] Other partially evolved GUS variants isolated during the *in vitro* evolution could not be investigated because their relatively low substrate turnover rates cannot be detected in the femtoliter array. Furthermore, it would have been interesting to analyze the newly evolved enzyme function by using galactoside substrates. However, even the activity of the best evolved GUS variant (T509A/S557P/N566S/K567Q) was too low to be detectable at the single molecule level (k_{cat}/K_M = 200 s^{-1} M^{-1} in the reaction with pNP galactoside).[23]

Figure 5 shows that the single molecule substrate turnover rates of partially evolved GUS variant T509A/D531E/S557P/N566S are long-lived, which has also been observed for individual molecules of wild-type GUS (Figure 3). The activity in a population of partially evolved GUS molecules, however, is significantly more broadly distributed (CV = 35%) compared to the wild-type activity investigated at 100 μM ReG (CV = 20%, Figure 5B) or any other substrate concentration (Figure 4). The broader activity distribution among individual enzyme molecules strongly indicates that partially evolved GUS can adopt a larger number of stable conformational states than wild-type GUS. Frauenfelder et al.[33] proposed the picture of a rugged energy landscape for proteins, in which conformational substates with different structural and dynamic properties are organized in a coarse hierarchy. According to this view, there are fast transitions between higher tiers that are separated by a low energy barrier and slow transitions in lower tiers separated by a high energy barrier. Even in the relatively small protein myoglobin three distinct taxonomic substates were found.[33] Protein folding is typically described as a folding funnel, where the horizontal plane depicts the conformational freedom and the vertical axis the free energy. A higher conformational heterogeneity can thus be explained by a wider folding funnel of partially evolved GUS compared to wild-type GUS. The surface of the folding funnel of evolved GUS can keep its rugged topography but in each local minimum more conformational substates can be accommodated. The long-lived and broadly distributed activity states indicate a "division of work" among the members of an enzyme population that accounts for the functional promiscuity of the generalist. This functional specialization of individual molecules as a motor for protein dynamism and evolvability[34,35] stands in stark contrast to the traditional view of proteins that possess absolute functional specificity mediated by a single fixed structure.[36]

It is important to note that the static heterogeneity does not rule out a larger number of dynamic transitions at higher tiers of the hierarchy, but these cannot be resolved with the time resolution of our experiment. A higher conformational plasticity could additionally lead to individual enzyme molecules that switch between different conformational states over time (dynamic heterogeneity)[6] and thus could perform different

catalytic functions. We suggest that the observed wider static heterogeneity is only the "tip of the iceberg" and transitions at lower tiers are at least equally important for the functional heterogeneity of partially evolved GUS. Other types of single molecule experiments, however, will be necessary to resolve such faster transitions.

The conformational flexibility of a protein is closely related to its thermostability because there is a trade-off between structural stability and the flexibility required to perform a catalytic function.[37] The strong impact of a few amino acid substitutions on the thermostability of GUS has already been demonstrated.[38,39] We analyzed changes in the secondary structure at elevated temperatures by circular dichroism (CD, SI Figures 6 and 7). As wild-type GUS and partially evolved GUS differ in only four (T509A/S557P/N566S/K567Q) of 603 amino acids (Figure 1A) they adopt a very similar secondary structure at ambient temperature. Increasing the temperature to more than 60 °C leads to a minor change in the secondary structure of wild-type GUS, which can be attributed to tetramer dissociation and is accompanied by a loss of enzymatic activity.[38] The overall secondary structure, however, remains largely unchanged up to 100 °C, thus indicating highly thermostable monomer subunits. In contrast, partially evolved GUS shows a typical thermal denaturation profile at temperatures higher than 60 °C, which is indicative of monomer unfolding. As a lower thermostability is a sign of higher conformational flexibility, we conclude that the more flexible conformation of the generalist is implicated in the broader activity distribution.

Finally, our study provides a glimpse at the evolution of primordial enzymes. According to the "patchwork" hypothesis first proposed by Ycas[40] and Jensen,[41] primordial enzymes possessed a very broad substrate specificity that offered ancient cells with minimal gene content a highly flexible metabolism. Later, gene duplication provided the basis for an increasing diversification and specialization of enzymatic activities. Together with the recruitment of regulation mechanisms, these steps gradually have led to the highly efficient metabolism that we know from modern cells. We suggest that the division of work observed among individual molecules of an enzyme population enabled ancient cells to compensate for their low gene content. The ability of an enzyme with a single amino acid sequence to adopt distinct and long-lived conformational states that catalyze various substrates allowed for an optimal use of the limited cellular resources. Only later was the catalytic information stored in the conformational space of individual enzyme molecules delegated to the RNA or DNA level to avoid disadvantageous side reactions in a more complex cellular environment. With this transfer of information, the promiscuous activity of enzymes became obsolete if not dangerous such that most—but not all[42]—modern enzymes evolved to adopt a more homogeneous activity.

■ CONCLUSION

We have demonstrated that single molecule experiments in femtoliter arrays provide new insights not only into the catalysis of enzymes but also how new catalytic activities evolve. β-Glucuronidase (GUS) catalyzes a simple hydrolytic reaction with high activity that can be readily observed at the single molecule level and compared to the closely related enzyme β-galactosidase. Both enzymes display long-lived but distinct individual substrate turnover rates and their mean activities are consistent with traditional Michaelis—Menten kinetics. Com-

pared to GUS, the activity of individual β-galactosidase molecules is more broadly distributed within the enzyme population,[15] which may be attributed to the broader range of reactions catalyzed by β-galactosidase. A broader activity distribution has also been observed for partially evolved GUS variant T509A/D531E/S557P/N566S that was isolated during the *in vivo* evolution of GUS into a β-galactosidase and hydrolyzes many different substrates.[23] The broad static heterogeneity found among individual substrate turnover rates of the generalist may be related to an ancient evolutionary mechanism that helped primordial cells to survive in spite of a low gene content.

ASSOCIATED CONTENT

Ⓢ Supporting Information

One video of single molecule substrate turnover in femtoliter chambers, seven figures, and two tables supporting the Experimental Section and Results and Discussion. This material is available free of charge via the Internet at http://pubs.acs.org.

AUTHOR INFORMATION

Corresponding Author
*Tel.: +49-941-943-4015. Fax: +49-941-943-4064. E-mail: hans-heiner.gorris@ur.de.

Present Address
Max Renner, Division of Structural Biology, University of Oxford, Oxford, United Kingdom.

Notes
The authors declare no competing financial interest.

ACKNOWLEDGMENTS

REFERENCES

(1) Michaelis, L.; Menten, M. L. *Biochem. Z.* **1913**, *49*, 333−369.
(2) Lu, H. P.; Xun, L.; Xie, X. S. *Science* **1998**, *282*, 1877−1882.
(3) Edman, L.; Földes-Papp, Z.; Wennmalm, S.; Rigler, R. *Chem. Phys.* **1999**, *247*, 11−22.
(4) Flomenbom, O.; Velonia, K.; Loos, D.; Masuo, S.; Cotlet, M.; Engelborghs, Y.; Hofkens, J.; Rowan, A. E.; Nolte, R. J.; Van der Auweraer, M.; de Schryver, F. C.; Klafter, J. *Proc. Natl. Acad. Sci. U. S. A.* **2005**, *102*, 2368−2372.
(5) Velonia, K.; Flomenbom, O.; Loos, D.; Masuo, S.; Cotlet, M.; Engelborghs, Y.; Hofkens, J.; Rowan, A. E.; Klafter, J.; Nolte, R. J. M.; de Schryver, F. C. *Angew. Chem., Int. Ed.* **2005**, *44*, 560−564.
(6) English, B. P.; Min, W.; van Oijen, A. M.; Lee, K. T.; Luo, G.; Sun, H.; Cherayil, B. J.; Kou, S. C.; Xie, X. S. *Nat. Chem. Biol.* **2006**, *2*, 87−94.
(7) De Cremer, G.; Roeffaers, M. B.; Baruah, M.; Sliwa, M.; Sels, B. F.; Hofkens, J.; De Vos, D. E. *J. Am. Chem. Soc.* **2007**, *129*, 15458−15459.
(8) Terentyeva, T. G.; Engelkamp, H.; Rowan, A. E.; Komatsuzaki, T.; Hofkens, J.; Li, C. B.; Blank, K. *ACS Nano* **2012**, *6*, 346−354.
(9) Rotman, B. *Proc. Natl. Acad. Sci. U. S. A.* **1961**, *47*, 1981−1991.
(10) Hsin, T. M.; Yeung, E. S. *Angew. Chem., Int. Ed* **2007**, *46*, 8032−8035.
(11) Gorris, H. H.; Blicharz, T. M.; Walt, D. R. *FEBS J.* **2007**, *274*, 5462−5470.
(12) Tan, W. H.; Yeung, E. S. *Anal. Chem.* **1997**, *69*, 4242−4248.
(13) Rondelez, Y.; Tresset, G.; Tabata, K. V.; Arata, H.; Fujita, H.; Takeuchi, S.; Noji, H. *Nat. Biotechnol.* **2005**, *23*, 361−365.
(14) Gorris, H. H.; Walt, D. R. *Angew. Chem., Int. Ed* **2010**, *49*, 3880−3895.
(15) Rissin, D. M.; Gorris, H. H.; Walt, D. R. *J. Am. Chem. Soc.* **2008**, *130*, 5349−5353.
(16) Gorris, H. H.; Rissin, D. M.; Walt, D. R. *Proc. Natl. Acad. Sci. U. S. A.* **2007**, *104*, 17680−17685.
(17) Gorris, H. H.; Walt, D. R. *J. Am. Chem. Soc.* **2009**, *131*, 6277−6282.
(18) Ehrl, B. N.; Liebherr, R. B.; Gorris, H. H. *Analyst* **2013**, *138*, 4260−4265.
(19) Jacobson, R. H.; Zhang, X. J.; DuBose, R. F.; Matthews, B. W. *Nature* **1994**, *369*, 761−766.
(20) Wallace, B. D.; Wang, H. W.; Lane, K. T.; Scott, J. E.; Orans, J.; Koo, J. S.; Venkatesh, M.; Jobin, C.; Yeh, L. A.; Mani, S.; Redinbo, M. R. *Science* **2010**, *330*, 831−835.
(21) Henrissat, B. *Biochem. J.* **1991**, *280*, 309−316.
(22) Jefferson, R. A.; Burgess, S. M.; Hirsh, D. *Proc. Natl. Acad. Sci. U. S. A.* **1986**, *83*, 8447−8451.
(23) Matsumura, I.; Ellington, A. D. *J. Mol. Biol.* **2001**, *305*, 331−339.
(24) Aharoni, A.; Gaidukov, L.; Khersonsky, O.; Gould, S. M.; Roodveldt, C.; Tawfik, D. S. *Nat. Genet.* **2005**, *37*, 73−76.
(25) Khersonsky, O.; Tawfik, D. S. *Annu. Rev. Biochem.* **2010**, *79*, 471−505.
(26) Claren, J.; Malisi, C.; Hocker, B.; Sterner, R. *Proc. Natl. Acad. Sci. U. S. A.* **2009**, *106*, 3704−3709.
(27) Pervushin, K.; Vamvaca, K.; Vogeli, B.; Hilvert, D. *Nat. Struct. Mol. Biol.* **2007**, *14*, 1202−1206.
(28) Bradford, M. M. *Anal. Biochem.* **1976**, *72*, 248−254.
(29) Pace, C. N.; Vajdos, F.; Fee, L.; Grimsley, G.; Gray, T. *Protein Sci.* **1995**, *4*, 2411−2423.
(30) Raouda, N.; Upert, G.; Angelici, G.; Nicolet, S.; Schmidt, T.; Schwede, T.; Creus, M. *Metallomics* **2014**, *6*, 88−95.
(31) Juers, D. H.; Matthews, B. W.; Huber, R. E. *Protein Sci.* **2012**, *21*, 1792−1807.
(32) Novel, G.; Didier-Fichet, M. L.; Stoeber, F. *J. Bacteriol.* **1974**, *120*, 89−95.
(33) Frauenfelder, H.; Sligar, S. G.; Wolynes, P. G. *Science* **1991**, *254*, 1598−1603.
(34) Tokuriki, N.; Tawfik, D. S. *Science* **2009**, *324*, 203−207.
(35) Peisajovich, S. G.; Tawfik, D. S. *Nat. Methods* **2007**, *4*, 991−994.
(36) James, L. C.; Tawfik, D. S. *Trends Biochem. Sci.* **2003**, *28*, 361−368.
(37) Vihinen, M. *Protein Eng.* **1987**, *1*, 477−480.
(38) Flores, H.; Ellington, A. D. *J. Mol. Biol.* **2002**, *315*, 325−337.
(39) Xiong, A. S.; Peng, R. H.; Cheng, Z. M.; Li, Y.; Liu, J. G.; Zhuang, J.; Gao, F.; Xu, F.; Qiao, Y. S.; Zhang, Z.; Chen, J. M.; Yao, Q. H. *Protein Eng. Des. Sel.* **2007**, *20*, 319−325.
(40) Ycas, M. *J. Theor. Biol.* **1974**, *44*, 145−160.
(41) Jensen, R. A. *Annu. Rev. Microbiol.* **1976**, *30*, 409−425.
(42) O'Brien, P. J.; Herschlag, D. *Chem. Biol.* **1999**, *6*, R91−R105.